

Nucleophilic Aromatic Substitution on Aryl-Amido Ligands Promoted by Oxidizing Osmium(IV) Centers

Jake D. Soper, Erik Saganic, David Weinberg, David A. Hrovat, Jason B. Benedict,[†] Werner Kaminsky,[†] and James M. Mayer*

Department of Chemistry, Campus Box 351700, University of Washington, Seattle, Washington 98195-1700

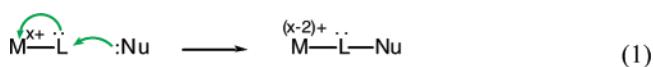
Received January 30, 2004

Addition of amine nucleophiles to acetonitrile solutions of the Os^{IV} anilido complex TpOs(NHPh)Cl₂ (**1**) [Tp = hydrotris(1-pyrazolyl)borate] gives products with derivatized anilido ligands, i.e., TpOs[NH-*p*-C₆H₄(N(CH₂)₅)]Cl₂ (**2**) from piperidine and TpOs[NH-*p*-C₆H₄N(CH₂)₄]Cl₂ (**3**) from pyrrolidine. These materials are formed in ~30% yield under anaerobic conditions, together with ~60% yields of the Os^{III} aniline complex TpOs(NH₂Ph)Cl₂ (**5**). Formation of the *para*-substituted materials **2** or **3** from **1** involves oxidative removal of two hydrogen atoms (two H⁺ and two e⁻). The oxidation can be accomplished by **1**, forming **5**, or by O₂. Related reactions have been observed with other amines and with the 2-naphthylamido derivative, which gives an *ortho*-substituted product. Kinetic studies indicate an addition–elimination mechanism involving initial attack of the amine nucleophile on the anilido ligand. These are unusual examples of nucleophilic aromatic substitution of hydrogen. Ab initio calculations on **1** show that the LUMO has significant density at the *ortho* and *para* positions of the anilido ligand, resembling the LUMO of nitrobenzene. By analogy with nucleophilic aromatic substitution, **2** is quantitatively formed from piperidine and the *p*-chloroanilide TpOs(NH-*p*-C₆H₄Cl)Cl₂ (**7**). Binding the anilide ligands to an oxidizing Os^{IV} center thus causes a remarkable umpolung or inversion of chemical character from a typically electron-rich anilido to an electron-deficient aromatic functionality. This occurs because of the coupling of redox changes at the TpOs^{IV} center with bond formation at the coordinated ligand.

Introduction

The reaction chemistry of well-characterized transition metal complexes that are strongly oxidizing has in general received less attention than related reactions of highly reducing compounds (with the exception of electron-transfer reactions).¹ This is perhaps surprising given the importance of metal-mediated oxidations in organic synthesis, in industrial processes, and in biochemical transformations.² One type of metal-mediated oxidations involves nucleophilic attack on a ligand bound to an oxidizing metal center. A classic example is the attack of a phosphine nucleophile on an oxo or nitrido ligand.³ Ligands with formally closed-shell electronic configurations are transformed into electrophiles by the oxidizing metal center, as shown schematically in eq 1. This is an inversion of the normal chemical character of the

ligand, an umpolung,⁴ because ligands are typically Lewis bases that bind to a Lewis acidic metal center.



Our approach to isolate and study oxidizing metal complexes complements the extensive work on catalytic oxidations, in which the active oxidant is generated in situ and is often difficult to observe and fully characterize. We and others have been examining oxidizing Os^{VIII}, Os^{VI}, and Os^{IV} complexes.^{5–7} The oxidizing osmium centers can activate ligands toward nucleophilic attack, most commonly the oxo and nitrido ligands that dominate the chemistry of the higher oxidation states.⁸ We have reported, for instance, that aryl anions add to the electrophilic nitrido ligand in the Os^{VI} complex TpOs(N)Cl₂ [Tp = hydrotris(1-pyrazolyl)borate], yielding arylamido complexes TpOs(NHAr)Cl₂.^{5a}

Reported here are reactions in which these arylamido ligands bound to osmium(IV) act as electrophiles: amines

* Author to whom correspondence should be addressed. E-mail: mayer@chem.washington.edu.

[†] University of Washington Crystallographic Facility.

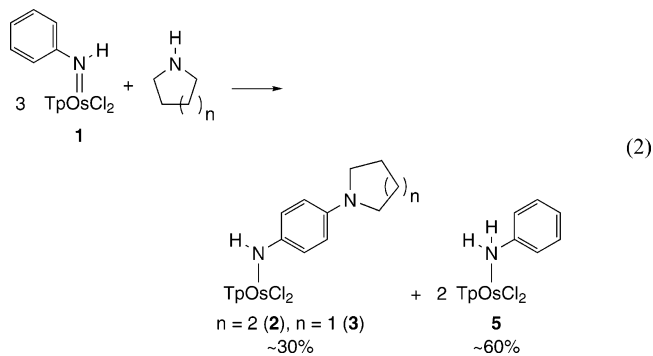
add to their aromatic rings in processes that resemble organic nucleophilic aromatic substitution.⁹ This is in contrast to the normal electron-rich character of anilido and amido ligands (R_2N^-), which are readily protonated and can be susceptible to electrophilic attack.¹⁰ Bound to the oxidizing $TpOs^{IV}$

center, however, the $NHAr$ ligand is a weaker base than triflate in acetonitrile.^{11,12} The Os^{IV} centers described herein are sufficiently electron-withdrawing to activate the anilido ligands, but they are not strong outer-sphere oxidants. Reduction of $TpOs(NHPh)Cl_2$ (**1**) occurs with $E_{1/2} = -1.05$ V vs $Cp_2Fe^{+/0}$ in CH_3CN .¹¹ The redox potential is not a good indicator of bond-forming reactivity. Reduction of osmium(IV) is much more favorable when coupled to reaction at the $NHAr$ ligand, either by nucleophile addition to the aromatic ring as described here or by protonation at the amido nitrogen. Such a proton-coupled electron transfer (PCET) can also be called hydrogen atom (H^\bullet) transfer. The ability of these osmium complexes to accept H^\bullet has been discussed elsewhere^{12,13} and is a critical part of the reactions described here. This report describes the scope and mechanism of these unusual reactions and the implications for this class of metal-mediated oxidation processes.

Results

Reaction of $TpOs(NHPh)Cl_2$ (**1**) with Secondary Amines.

Addition of 3 equiv of piperidine to solutions of $TpOs(NHPh)Cl_2$ (**1**) in CH_3CN gives a color change from dark red to bright blue over days at ambient temperatures. 1H NMR spectra of the blue solutions do not show formation of deprotonated $[TpOs(NPh)Cl_2]^-$ (characterized previously as its MgX^+ salt)¹¹ but instead show two osmium products, **2** and **5** (eq 2). Reaction of **1** with pyrrolidine under the same



conditions gives similar results, forming **3** and **5**. The major product in each case, **5** (~60% by integration versus an internal standard), is barely evident in the 1H NMR spectra because its resonances are broad and paramagnetically shifted (δ 64 to -51 ppm, full-width half-maximum (fwhm) 68–1100 Hz).¹⁴ Complex **5** has been shown to be the Os^{III} aniline complex $TpOs(NH_2Ph)Cl_2$ by independent synthesis and crystallographic characterization, as reported elsewhere.¹³ Clean isolation of **5** from this reaction is challenging because of its air sensitivity, readily converting to **1** in air in the presence of base or on silica gel.¹³

- (1) For examples of strongly reducing chemistry, see: (a) Cummins, C. C. In *Progress in Inorganic Chemistry*; Karlin, K. D. Ed.; Wiley: New York, 1998; Vol. 47, pp 685–836. (b) Cherry, J.-P. F.; Johnson, A. R.; Baraldo, L. M.; Tsai, Y.-C.; Cummins, C. C.; Kyatov, S. V.; Rybak-Akimova, E. V.; Capps, K. B.; Hoff, C. D.; Harr, C. M.; Nolan, S. P. *J. Am. Chem. Soc.* **2001**, *123*, 7271–7286. (c) Fryzuk, M. D.; Johnson, S. A.; Patrick, B. O.; Albinati, A.; Mason, S. A.; Koetzle, T. F. *J. Am. Chem. Soc.* **2001**, *123*, 3960–3973. (d) Evans, W. J.; Allen, N. T.; Ziller, J. W. *J. Am. Chem. Soc.* **2001**, *123*, 7927–7928. (e) Harman, W. D. *Chem. Rev.* **1997**, *97*, 1953–1978. (f) Maseras, F.; Lockwood, M. A.; Eisenstein, O.; Rothwell, I. P. *J. Am. Chem. Soc.* **1998**, *120*, 6598–6602. (g) Yandulov, D. V.; Schrock, R. R. *Science* **2003**, *301*, 76–78. (h) Veige, A. S.; Slaughter, L. M.; Lobkovsky, E. B.; Wolczanski, P. T.; Matsunaga, N.; Decker, S. A.; Cundari, T. R. *Inorg. Chem.* **2003**, *42*, 6204–6224. (i) Berube, C. D.; Gambarotta, S.; Yap, G. P. A.; Cozzi, P. G. *Organometallics* **2003**, *22*, 434–439. (j) Mayer, J. M. In *Advances in Transition Metal Coordination Chemistry*; Che, C.-M., Yam, V. W.-W., Eds.; JAI Press: Greenwich CN, 1996; Vol. 1, pp 105–157.
- (2) (a) Sheldon, R. A.; Kochi, J. K. *Metal-Catalyzed Oxidation of Organic Compounds*; Academic: New York, 1981. (b) Stewart, R. *Oxidation Mechanisms*; Benjamin: New York, 1964. (c) Olah, G. A.; Molnar, A. *Hydrocarbon Chemistry*; Wiley: New York, 1995. (d) *Organic Syntheses by Oxidation with Metal Compounds*; Mijs, W. J., de Jong, C. R. H. L., Eds.; Plenum: New York, 1986. (e) *Biomimetic Oxidations Catalyzed by Transition Metal Complexes*; Meunier, B., Ed.; Imperial College: London, 2000. (f) Beller, M.; Sharpless, K. B. In *Applied Homogeneous Catalysis with Organometallic Compounds*, 2nd ed.; Cornils, B., Herrmann, W., Eds.; Wiley-VCH: New York, 2002; Vol. 3, pp 1149–1164. (g) Sharpless, K. B. *Angew. Chem., Int. Ed.* **2002**, *41*, 2024–2032. (h) Jacobsen, E. N. In *Comprehensive Organometallic Chemistry II*; Wilkinson, G., Stone, F. G. A., Abel, E. W., Hegedus, L. S., Eds.; Pergamon: New York, 1995; Vol. 12, pp 1097–1135. (i) Cowan, J. A. *Inorganic Biochemistry: An Introduction*; Wiley-VCH: New York, 1997.
- (3) Nugent, W. A.; Mayer, J. M. *Metal Ligand Multiple Bonds*; Wiley: New York, 1988.
- (4) Seebach, D. *Angew. Chem., Int. Ed. Engl.* **1979**, *18*, 239–258.
- (5) (a) Crevier, T. J.; Bennett, B. K.; Soper, J. D.; Bowman, J. A.; Dehestani, A.; Hrovat, D. A.; Lovell, S.; Kaminsky, W.; Mayer, J. M. *J. Am. Chem. Soc.* **2001**, *123*, 1059–1071. (b) Bennett, B. K.; Lovell, S.; Mayer, J. M. *J. Am. Chem. Soc.* **2001**, *123*, 4336–4337. (c) McCarthy, M. R.; Crevier, T. J.; Bennett, B. K.; Dehestani, A.; Mayer, J. M. *J. Am. Chem. Soc.* **2000**, *122*, 12391–12392. (d) Bennett, B. K.; Saganic, E.; Lovell, S.; Kaminsky, W.; Samuel, A.; Mayer, J. M. *Inorg. Chem.* **2003**, *42*, 4127–4134. (e) Crevier, T. J.; Mayer, J. M. *Angew. Chem., Int. Ed.* **1998**, *37*, 1891–1893. (f) Dehestani, A.; Kaminsky, W.; Mayer, J. M. *Inorg. Chem.* **2003**, *42*, 605–611.
- (6) (a) Meyer, T. J.; Huynh, M. H. V. *Inorg. Chem.* **2003**, *42*, 8140–8160 and references therein. (b) Pipes, D. W.; Bakir, M.; Vitols, S. E.; Hodgson, D. J.; Meyer, T. J. *J. Am. Chem. Soc.* **1990**, *112*, 5507. (c) Demadis, K. D.; El-Samanody, E.-S.; Meyer, T. J.; White, P. S. *Inorg. Chem.* **1998**, *37*, 838–839. (d) Huynh, M. H. V.; Lee, D. G.; White, P. S.; Meyer, T. J. *Inorg. Chem.* **2001**, *40*, 3842–3849. (e) Huynh, M. H. V.; El-Samanody, E.-S.; Demadis, K. D.; Meyer, T. J.; White, P. S. *J. Am. Chem. Soc.* **1999**, *121*, 1403–1404. (f) Huynh, M. H. V.; Meyer, T. J.; *Angew. Chem., Int. Ed.* **2002**, *41*, 1395–8. (g) Huynh, M. H. V.; Lee, D. G.; White, P. S.; Meyer, T. J. *J. Am. Chem. Soc.* **1999**, *121*, 10446–10447.
- (7) (a) Che, C.-M.; Yam, V. W.-W. In *Advances in Inorganic Chemistry*; Sykes, A. G., Ed.; Academic Press: New York, 1992; Vol. 39, pp 233–325. (b) Marshman, R. W.; Shapley, P. A. *J. Am. Chem. Soc.* **1990**, *112*, 8369. (c) Schwab, J. J.; Wilkinson, E. C.; Wilson, S. R.; Shapley, P. A. *J. Am. Chem. Soc.* **1991**, *113*, 6124–6129. (d) Chan, P.-M.; Yu, W.-Y.; Che, C.-M.; Cheung, K.-K. *J. Chem. Soc., Dalton Trans.* **1998**, 3183–3190. (e) Maestri, A. G.; Cherry, K. S.; Toboni, J. J.; Brown, S. N. *J. Am. Chem. Soc.* **2001**, *123*, 7459–7460. (f) Brown, S. N. *J. Am. Chem. Soc.* **1999**, *121*, 9752–9753.
- (8) Griffith, W. P. Osmium. In *Comprehensive Coordination Chemistry*; Wilkinson, G., Ed.; Pergamon: New York, 1987; Vol. 4, pp 519–633.
- (9) Portions of this work have been previously communicated: Soper, J. D.; Kaminsky, W.; Mayer, J. M. *J. Am. Chem. Soc.* **2001**, *123*, 5594–5595.

- (10) (a) Lappert, M. F.; Power, P. P.; Sanger, A. R.; Srivastava, R. C. *Metal and Metalloid Amides*; Wiley: New York, 1980. (b) See, for example, ref 30 and Fulton, J. R.; Sklenak, S.; Bouwkamp, M. W.; Bergman, R. G. *J. Am. Chem. Soc.* **2002**, *124*, 4722–4737.
- (11) Soper, J. D.; Bennett, B. K.; Lovell, S.; Mayer, J. M. *Inorg. Chem.* **2001**, *40*, 1888–1893.
- (12) Soper, J. D.; Mayer, J. M. *J. Am. Chem. Soc.* **2003**, *125*, 12 217–12 229.
- (13) Soper, J. D.; Rhile, I. J.; DiPasquale, A. G.; Mayer, J. M. *Polyhedron* **2004**, *23*, 323–329.

Table 1. X-ray Diffraction Data for $\text{TpOs}[\text{NH-}p\text{-C}_6\text{H}_4(\text{N}(\text{CH}_2)_5)]\text{Cl}_2 \cdot \text{Acetone}$ (**2**·acetone), $\text{TpOs}[\text{NH-}p\text{-C}_6\text{H}_4(\text{N}(\text{CH}_2)_4)]\text{Cl}_2 \cdot \text{CD}_3\text{CN}$ (**3**· CD_3CN), and $\text{TpOs}[\text{NH-(2-naphthyl-1-piperidine)}]\text{Cl}_2$ (**10**)

complex	2 ·acetone	3 · CD_3CN	10
empirical formula	$\text{C}_{23}\text{H}_{31}\text{BCl}_2\text{N}_8\text{Os}$	$\text{C}_{21}\text{H}_{26}\text{BCl}_2\text{N}_9\text{Os}$	$\text{C}_{24}\text{H}_{27}\text{BCl}_2\text{N}_8\text{Os}$
FW	707.47	676.42	699.45
crystal system	monoclinic	monoclinic	monoclinic
space group	$P2_1/c$	$P2_1/n$	$P2_1/c$
unit cell dimensions (Å, deg)	$a = 12.1960(3)$ $b = 22.0420(11)$ $c = 16.8890(6)$ $\beta = 143.526(3)$	$a = 8.6030(3)$ $b = 27.533(11)$ $c = 10.4560(3)$ $\beta = 97.632(2)$	$a = 11.8650(5)$ $b = 11.9320(5)$ $c = 18.6910(8)$ $\beta = 104.236(2)$
volume (Å ³)	2698.99(26)	2454.74(15)	2564.88(19)
Z	4	4	4
density (g/cm ³ , calcd)	1.741	1.830	1.811
μ (mm ⁻¹)	4.955	5.442	5.211
λ (Å)	0.71070	0.71070	0.71070
crystal size (mm ³)	$0.60 \times 0.18 \times 0.06$	$0.24 \times 0.22 \times 0.10$	$0.24 \times 0.17 \times 0.05$
temperature (K)	293(2)	130(2)	130(2)
θ range (deg)	3.38–28.34	2.46–24.74	2.88–28.30
index ranges	$-16 \leq h \leq 16$ $-29 \leq k \leq 29$ $-22 \leq l \leq 12$	$-8 \leq h \leq 10$ $-30 \leq k \leq 32$ $-12 \leq l \leq 12$	$-15 \leq h \leq 15$ $-15 \leq k \leq 14$ $-24 \leq l \leq 23$
reflections collected	11052	6976	9606
unique reflections	6534	3987	5971
R_{int}	0.083	0.035	0.080
parameters refined	334	317	326
final R , R_w ($I > 2\sigma I$)	0.044, 0.088	0.032, 0.073	0.044, 0.085
goodness of fit	0.977	1.006	0.999

Compounds **2** and **3** are also paramagnetic, but their much smaller range of chemical shifts (δ 1.7–16 ppm) and fairly sharp resonances (fwhm \cong 4 Hz) make them much more evident in the ¹H NMR spectra despite their lower yield of ~30%. The sharpness and the small paramagnetic shifts are typical of third-row d⁴ octahedral complexes.^{5,15,16} Complexes **2** and **3** are isolated by column chromatography on silica gel in air and recrystallized from acetone/pentane. To our surprise, single-crystal X-ray diffraction showed these materials to be $\text{TpOs}[\text{NH-}p\text{-C}_6\text{H}_4(c\text{-N}(\text{CH}_2)_5)]\text{Cl}_2$ (**2**) and $\text{TpOs}[\text{NH-}p\text{-C}_6\text{H}_4(c\text{-N}(\text{CH}_2)_4)]\text{Cl}_2$ (**3**) with a piperidiny or pyrrolidiny substituent in place of hydrogen at the *para* position of the anilido ring. Compound **1** is written with an Os^{IV}=N bond because significant multiple bond character has been found,^{11,12} but the bonding in **2** and **3** is more complicated, as discussed below.

Addition of morpholine to **1** affords the related product $\text{TpOs}[\text{NH-}p\text{-C}_6\text{H}_4(c\text{-NC}_4\text{H}_8\text{O})]\text{Cl}_2$ (**4**), though the reaction is slow and heating an NMR reaction at 80 °C for 11 days is required for complete color change to bright blue at the same concentrations. No reaction is observed with diethylamine under similar conditions. ¹H NMR spectra in CD₃CN for **2–4** are all consistent with octahedral TpOs^{IV} compounds of *C_s* symmetry. These compounds are blue because of intense absorptions ca. 600 nm, $\epsilon \approx 25,000 \text{ M}^{-1} \text{ cm}^{-1}$ (see Figures S1 and S2 in Supporting Information).

The solid-state structures of **2**·acetone and **3**·CD₃CN both contain isolated molecules with pseudo-octahedral coordination (Tables 1 and 2, Figure 1). The osmium-anilido bond lengths, Os–N(7) = 1.945(7) (**2**) and 1.922(5) (**3**) Å, are similar to that in **1**, 1.919(6) Å, and to those in related Os^{IV} species.^{5,11,12,17} In contrast, Os^{III} aniline derivatives have ca. 0.2 Å longer bonds because they have formally dative Os ← N interactions.^{12,13} Compounds **2** and **3** may therefore be described as Os^{IV} anilido complexes with some Os–N(7) multiple-bond character, shown as **A** in Chart 1. However, the structural data also indicate a contribution from an Os^{II} quinone diimine resonance form (**B** in Chart 1), as has been suggested for related compounds.^{18,19} The α -carbons of the amine rings are coplanar with the aryl ring in both **2** and **3**, as required in the diimine form. In **2**, for instance, the C–C–N–C torsion angles are $-0.6(14)^\circ$ and $-4.3(15)^\circ$. Additionally, in both structures the “aromatic” C–C distances show small but consistent and statistically significant ($>2\sigma$) quinonoid-like alternations of long and short bonds around the ring (Table 2). In both **2** and **3**, the osmium center lies nearly in the plane of the aryl ring and N(7) [Os–N(7)–C(10)–C(11) dihedral angles of $172.2(6)^\circ$ (**2**) and $176.1(4)^\circ$ (**3**)], as required for π -delocalization. In form **A**, the anilido ligand serves as a π -donor to Os^{IV}, whereas in **B** the diazaquinone ligand can act as a π -acceptor for electron-rich d⁶ Os^{II}.²⁰ The intense optical transition at ~600 nm can thus be described as LMCT from the *p*-aminoanilido ligand to oxidizing Os^{IV} (from the perspective of resonance form

(14) Completed reactions of **1** with piperidine or pyrrolidine show resonances with ¹H NMR chemical shifts that match the spectrum of isolated **5**. The peak line widths for **5**, however, are broader in the reaction mixture as a result of degenerate proton self-exchange between **5** and trace $\text{TpOs}(\text{NHPH})\text{Cl}_2^-$ (**6**; generated in situ from **5** and the amine), as discussed elsewhere.¹² Removal of excess amine in vacuo and dissolution in CD₃CN gives a ¹H NMR spectrum that matches that of isolated **5**.

(15) (a) Randall, E. W.; Shaw, D. *J. Chem. Soc. A* **1969**, 2867–2872. (b) Chatt, J.; Leigh, G. J.; Mingos, D. M. P. *J. Chem. Soc. A* **1966**, 1674–1680.

(16) Bennett, B. K.; Pitteri, S. J.; Pilobello, L.; Lovell, S.; Kaminsky, W.; Mayer, J. M. *J. Chem. Soc., Dalton Trans.* **2001**, 3489–3497.

(17) Crevier, T. C. Ph.D. Thesis, University of Washington, 1998.

(18) Joss, S.; Bigler, P.; Ludi, A. *Inorg. Chem.* **1985**, *24*, 3487–3488.

(19) (a) Ghosh, A. K.; Peng, S.-M.; Paul, R. L.; Ward, M. D.; Goswami, S. *J. Chem. Soc., Dalton Trans.* **2001**, 336–340. (b) Mitra, K. N.; Choudhury, S.; Castineiras, A.; Goswami, S. *J. Chem. Soc., Dalton Trans.* **1998**, 2901–2906. (c) Mitra, K. N.; Goswami, S. *Inorg. Chem.* **1997**, *36*, 1322–1326. (d) Das, C.; Ghosh, A. K.; Hung, C.-H.; Lee, G.-H.; Peng, S.-M.; Goswami, S. *Inorg. Chem.* **2002**, *41*, 7125–7135 and references therein.

(20) Harman, W. D. *Chem. Rev.* **1997**, *97*, 1953–1978.

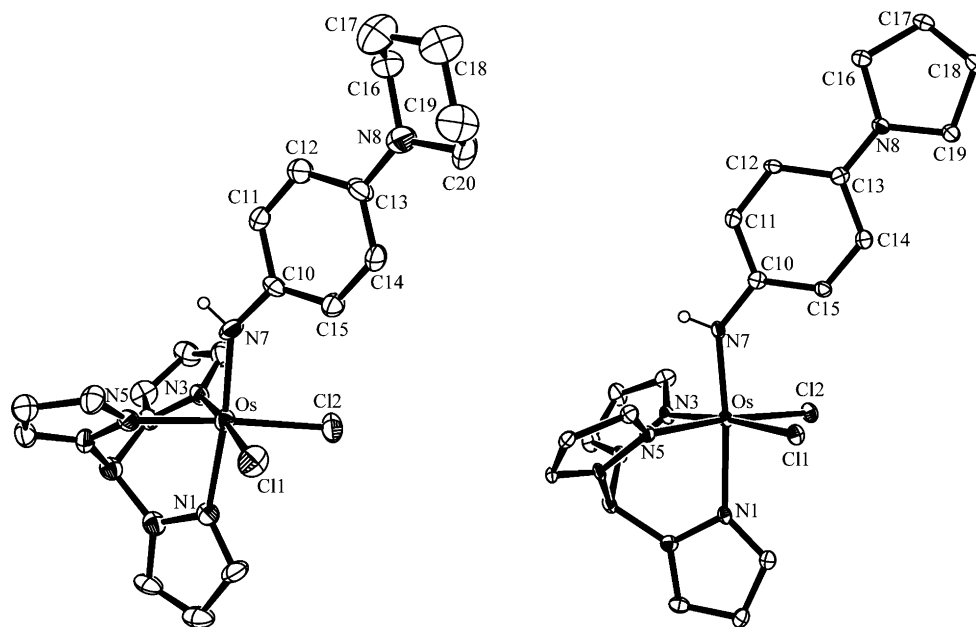


Figure 1. ORTEP drawings of $\text{TpOs}[\text{NH-}p\text{-C}_6\text{H}_4(\text{N}(\text{CH}_2)_5)]\text{Cl}_2$ (**2**) (left) and $\text{TpOs}[\text{NH-}p\text{-C}_6\text{H}_4(\text{N}(\text{CH}_2)_4)]\text{Cl}_2$ (**3**) (right). The solvent molecules are omitted for clarity.

Table 2. Selected Bond Lengths (Å), Angles, and Torsion Angles (deg) for $\text{TpOs}[\text{NH-}p\text{-C}_6\text{H}_4(\text{N}(\text{CH}_2)_5)]\text{Cl}_2 \cdot \text{Acetone}$ (**2**·acetone), $\text{TpOs}[\text{NH-}p\text{-C}_6\text{H}_4(\text{N}(\text{CH}_2)_4)]\text{Cl}_2 \cdot \text{CD}_3\text{CN}$ (**3**· CD_3CN), and $\text{TpOs}[\text{NH-(2-naphthyl-1-piperidine)}]\text{Cl}_2$ (**10**)

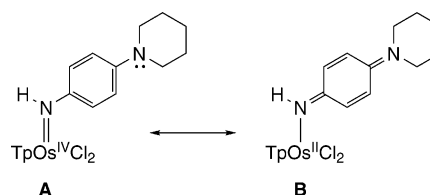
	2 ·acetone.	3 · CD_3CN	10 ^a
Os–N(1)	2.095(5)	2.081(4)	2.069(6)
Os–N(3)	2.056(5)	2.056(4)	2.057(4)
Os–N(5)	2.055(5)	2.054(4)	2.059(5)
Os–N(7)	1.951(6)	1.922(5)	1.926(6)
Os–Cl(1)	2.3786(17)	2.3801(12)	2.3657(15)
Os–Cl(2)	2.3749(14)	2.3834(12)	2.3540(13)
N(7)–C(10)	1.358(8)	1.371(6)	1.364(8)
C(10)–C(11)	1.405(9)	1.406(7)	1.431(8)
C(11)–C(12)	1.353(9)	1.393(7)	1.416(9)
C(12)–C(13)	1.426(8)	1.421(7)	1.432(8)
C(13)–C(14)	1.396(9)	1.428(7)	1.416(9)
C(14)–C(15)	1.369(9)	1.374(7)	1.372(9)
C(10)–C(15)	1.386(8)	1.408(7)	1.419(8)
N(8)–C(13)	1.377(9)	1.352(6)	1.421(7) ^c
N(8)–C(16)	1.494(9)	1.453(6)	1.466(7)
N(8)–C(20)	1.489(8)	1.463(6) ^b	1.463(8)
Cl(1)–Os–Cl(2)	90.88(6)	92.13(4)	92.51(5)
N(7)–Os–N(1)	172.9(2)	174.52(18)	174.5(2)
N(7)–Os–N(3)	88.8(2)	90.04(17)	90.8(2)
N(7)–Os–N(5)	90.0(2)	90.38(18)	88.7(2)
N(7)–Os–Cl(1)	95.15(16)	94.78(14)	93.7(2)
N(7)–Os–Cl(2)	94.05(15)	95.02(14)	95.0(2)
Os–N(7)–C(10)	139.2(4)	137.1(4)	138.6(4)
Os–N(7)–C(10)–C(11)	172.3(5)	–176.1(4)	–1.3(10)
Os–N(7)–C(10)–C(15)	–7.1(10)	3.2(8)	–1.9(7)
C(12)–C(13)–N(8)–C(16)	0.1(11)	–1.8(8)	–70.8(8) ^e
C(14)–C(13)–N(8)–C(20)	–5.1(11)	0.6(7) ^d	108.3(7) ^f

^a C(21)–C(22) 1.383(10), C(22)–C(23) 1.398(9), C(23)–C(24) 1.382(9), C(24)–C(13) 1.407(9). ^b N(8)–C(19). ^c N(8)–C(11). ^d C(14)–C(13)–N(8)–C(19). ^e C(10)–C(11)–N(8)–C(20). ^f C(12)–C(11)–N(8)–C(16).

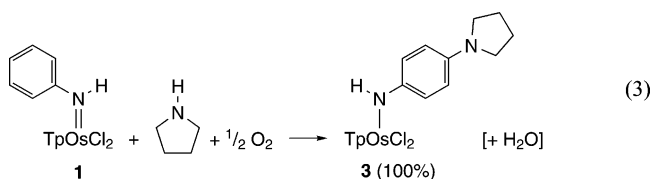
A) or as MLCT from reducing Os^{II} to the diazaquinone ligand (of form B).

Equation 2 is a balanced reaction: 3 equiv of **1** and a secondary amine yield 1 equiv of **2**, **3** or **4** plus 2 equiv of **5**. The products **2**–**4** have two fewer hydrogen atoms than **1** + amine, and transfer of these hydrogen atoms to two molecules of the starting material **1** forms two **5**. Since the

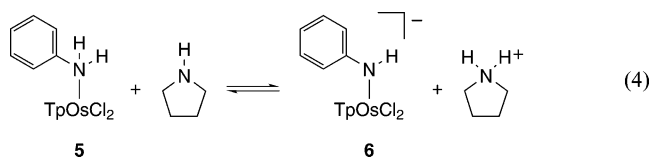
Chart 1



broad resonances of **5** make its yield difficult to quantify by NMR, the stoichiometry was confirmed by addition of O_2 to a completed reaction of **1** + piperidine. This converts **5** back to **1**, which is easily quantified by ^1H NMR (62%). Reaction of **1** with pyrrolidine under 1 atm O_2 for 19 d give stoichiometric conversion to **3** (by ^1H NMR) since **5** is recycled back to **1** (eq 3).



Kinetic Studies. Reactions of **1** with pyrrolidine, piperidine, and morpholine were monitored by UV–vis spectroscopy under anaerobic conditions in dry acetonitrile, usually with $4\text{--}6 \times 10^{-2}$ mM **1** and 40–200 mM amine. With pyrrolidine and piperidine, the reactions were typically complete in less than 24 h at 298 K. Final optical spectra of reactions of **1** with pyrrolidine indicate the presence of **3**, **5**, and the deprotonated form of **5**, $[\text{TpOs}(\text{NHPh})\text{Cl}_2]^-$ (**6**)¹² (Figures S1 and S2). Removal of excess pyrrolidine in vacuo



and dissolution in CH_3CN afford a spectrum characteristic of only **3** and **5**, since the equilibrium in eq 4 is shifted to **5** upon removal of base. The data are consistent with the reported $\text{p}K_{\text{a}}$ values for [**5**] (22.5 ± 0.1)¹³ and pyrrolidine (19.58 ± 0.05)²¹ in CH_3CN .

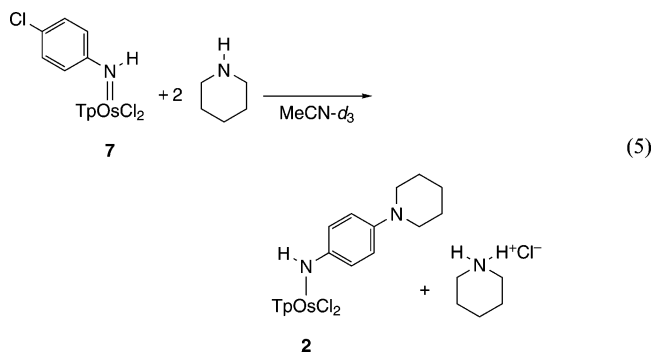
Global fitting of the spectra (250–700 nm) with SpecFit indicates pseudo-first-order kinetics under these conditions with excess amine. The first-order rate constants k_{obs} are independent of the initial concentration of **1** and are reproducible between different batches of **1** and CH_3CN . In studies at 25, 35, and 55 °C, k_{obs} varies fairly linearly with [pyrrolidine], although the plot of $k_{\text{obs}} = k[\text{NHR}_2] + c$ for the 25 °C data has a significant negative intercept (Figure S3). The data indicate that the reaction with pyrrolidine is first order in both amine and in **1** (although there may be a deviation at high [pyrrolidine]). The derived second-order rate constant for formation of **3** is $k_3 = (1.7 \pm 0.4) \times 10^{-3} \text{ M}^{-1} \text{ s}^{-1}$ at 298 K. Reactions of the deuterated materials $\text{TpOs}(\text{NHPh-}d_5)\text{Cl}_2$ (**1-}d_5) and pyrrolidine-1-*d* give $k_{3(\text{D})} = (2.0 \pm 0.3) \times 10^{-3} \text{ M}^{-1} \text{ s}^{-1}$ at 298 K, so the kinetic isotope effect is 1 within error. Rate constants for the reaction of **1** with pyrrolidine in CH_3CN are essentially independent of temperature, with values [$\times 10^{-3} \text{ M}^{-1} \text{ s}^{-1}$] of 1.7 ± 0.4 at 298 K, 1.7 ± 0.3 at 318 K, and 1.5 ± 0.3 at 328 K. Eyring analysis (25–55 °C) gives $\Delta H^\ddagger = -1 \pm 2 \text{ kcal mol}^{-1}$ and $\Delta S^\ddagger = -80 \pm 20 \text{ eu}$. The activation entropy is significantly more negative than expected for a typical, bimolecular reaction (ca. –20 to 40 eu).²² Treatment of **1** with pyrrolidine in mixed $\text{CH}_3\text{CN}/\text{benzene}$ (60/40) solvent gives similar spectral changes and a bimolecular rate constant, determined as described above, of $k_3 = (4.7 \pm 0.6) \times 10^{-4} \text{ M}^{-1} \text{ s}^{-1}$ at 298 K. The lower dielectric of the mixed solvent system slows the reaction by a factor of 4.**

The reaction of **1** with piperidine ($\text{p}K_{\text{a}} = 18.92 \pm 0.05$)²¹) is similar to that with pyrrolidine, in both the spectral changes and the kinetics. The bimolecular rate constant $k_2 = (7.4 \pm 0.9) \times 10^{-4} \text{ M}^{-1} \text{ s}^{-1}$ at 298 K is 2.7 times slower than k_3 . In contrast, the reaction with excess morpholine ($\text{p}K_{\text{a}} = 16.61 \pm 0.05$)²¹) is substantially slower, with complete conversion to **4** and **5** requiring months at 298 K. This reaction appears to occur in two kinetic phases, the first taking 3–7 days at the concentrations used, then a very slow phase to form product. An intermediate, less absorbing in the visible region than **1** or **4**, is apparently formed in the first phase. An attempt at isolation of the intermediate by removal of the excess morpholine yielded only **1**, suggesting that it is formed in an equilibrium process. The intermediate is not observed by NMR in the presence of a much lower morpholine concentration. The morpholine reaction, in contrast to the pyrrolidine case, proceeds faster upon heating, requiring only 11 days at 80 °C in an NMR tube to reach completion.

Reactions of $\text{TpOs}(\text{NHPh})\text{Cl}_2$ (1**) with Other Nucleophiles.** Exposure of **1** in CD_3CN to 1 atm methylamine gives a color change from dark red to purple over days at ambient

temperature. ^1H NMR spectra of reaction mixtures show formation of a new species with C_s symmetry and **5** in the expected ~30% and 60% yields. The C_s symmetric material was isolated by column chromatography on silica gel in air and found to be the *para*-substituted methylaminy product analogous to **2–4** by ^1H NMR spectroscopy. With the tertiary amine quinuclidine, reaction with **1** in CD_3CN for days at 80 °C gives a color change from dark red to bright blue, consistent with product(s) formed from some type of nucleophilic attack. ^1H NMR spectra and chromatography, however, show multiple Tp-containing products that could not be separated or characterized. No reaction is observed between **1** and pyridine, aniline, or diphenylamine after heating for weeks at 80 °C. Rapid reactions were observed between **1** and a variety of other nucleophiles, including benzyl mercaptan (which yielded some **5**), hydroxide, 3-chloroperoxybenzoic acid (*m*-CPBA), and *tert*-butyl hydroperoxide, but typically mixtures and/or NMR-silent products were formed.

Reactions of *p*-Chloroanilido and Other Anilido Complexes. Reaction 2 is formally a nucleophilic aromatic substitution ($\text{S}_{\text{N}}\text{Ar}$) of hydrogen.²³ Nucleophilic substitutions more typically displace halides or other good leaving groups. To test the analogy with organic $\text{S}_{\text{N}}\text{Ar}$ processes, the *p*-chloroanilido derivative $\text{TpOs}(\text{NH-}p\text{-C}_6\text{H}_4\text{Cl})\text{Cl}_2$ (**7**) was prepared. Heating excess 4-chloroaniline and $\text{TpOs}(\text{N})\text{Cl}_2$ in CH_2Cl_2 over 4 d at 80 °C gives **7** in low yield (15%) after chromatographic separation. This synthesis had been previously applied to the *p*-tolyl derivative;¹⁷ it may involve the aniline trapping a TpOsCl_2 fragment formed upon decomposition of $\text{TpOs}(\text{N})\text{Cl}_2$, which occurs on roughly the same time scale under these conditions. Anaerobic exposure of **7** to 3 equiv of piperidine in CD_3CN gives **2** in quantitative yield after ca. 10 weeks at ambient temperature (by ^1H NMR). Complete conversion to **2** is achieved without added oxidant because piperidine·HCl is formally the second product of the reaction (eq 5).



Ab initio calculations on **1** (vide infra) suggest that reaction could occur at both the *ortho* and *para* positions of the anilido ring. Experimentally, however, only *para*-substituted products are observed. The reaction of the *p*-methylanilido $\text{TpOs}(\text{NHTol})\text{Cl}_2$ ¹⁷ with pyrrolidine has been carried out in an attempt to force nucleophilic attack at the *ortho* position of the anilido ligand. Addition of pyrrolidine to $\text{TpOs}(\text{NHTol})\text{Cl}_2$ in CD_3CN gives a color change from dark red to bright

(21) Izutsu, K. *Acid-Base Dissociation Constants in Dipolar Aprotic Solvents*; Blackwell Scientific: Boston, 1990.

(22) Lowry, T. H.; Richardson, K. S. *Mechanism and Theory and Organic Chemistry*, 3rd ed.; HarperCollins: New York, 1987; pp 209–213.

blue over days at ambient temperatures. Although this is consistent with formation of ring-substituted materials, the osmium product(s) formed are NMR-silent and column chromatography gives several uncharacterized osmium-containing products in low yield.

The anilido-bis(triflate) complex $\text{TpOs}(\text{NHPh})(\text{OTf})_2$ (**8**)¹¹ reacts within time of mixing with secondary amines (pyrrolidine, piperidine, morpholine, and diethylamine), quinuclidine, and pyridine. The color change in CD_3CN from dark orange to bright blue suggests the formation of ring-substituted products, but ^1H NMR and chromatography indicate that a number of products are formed in each case. ^{19}F NMR of a reaction of **8** with pyrrolidine in CD_3CN shows loss of the covalent triflate resonance at -77.7 ppm (vs external CFCl_3) and appearance of the signal for ionic triflate at -78.8 ppm.²⁴ Apparently the triflate ligands are displaced by the amines. We have found TpOs^{IV} -triflate complexes to be substitution inert, so perhaps this substitution is occurring on a lower-valent material formed by nucleophilic attack (possibly an $\text{Os}^{\text{III}}(\text{NH}_2\text{Ph})$ complex or an Os^{II} species resembling resonance form **B** above).

Reactions of Naphthyl-Amido Complexes. 1-Naphthyl- and 2-naphthyl-amido complexes are prepared by addition of the appropriate naphthyl Grignard reagent to $\text{TpOs}(\text{N})\text{Cl}_2$ and chromatographic workup, analogous to a synthesis of **1**.^{5a} Their compositions are indicated by ^1H NMR, ESI/MS, and elemental analyses. Aerobic reaction of the purple 2-naphthyl derivative $\text{TpOs}[\text{NH}(2\text{-naphthyl})]\text{Cl}_2$ (**9**) with 1 equiv of piperidine for 1 week yields a dark green product, **10**, in 70% yield after chromatography and recrystallization. An X-ray crystal structure (Tables 1 and 2, Figure 2) shows that **10** has a piperidyl group in the 1-naphthyl position: $\text{TpOs}[\text{NH}(2\text{-naphthyl-1-piperidine})]\text{Cl}_2$. ^1H NMR and FAB^+/MS spectra are consistent with this assignment. As in the reactions of **1**, substitution of an aromatic hydrogen for piperidine has occurred. In this case, substitution occurs *ortho* to the amido nitrogen because the *para* position is blocked as part of the naphthyl ring.

The structure of **10** has an osmium-N(anilide) bond length of 1.926(6) Å, close to those in **2**, **3**, and related Os^{IV} complexes.^{5,11,12} Unlike the structures of **2** and **3**, however, the piperidine ring is roughly orthogonal to the naphthyl ring, as indicated by the C(10)–C(11)–N(8)–C(20) dihedral angle of 70.8(8)°. This places the lone pair of the piperidyl nitrogen in the arene plane, facing the osmium. Thus, **10**

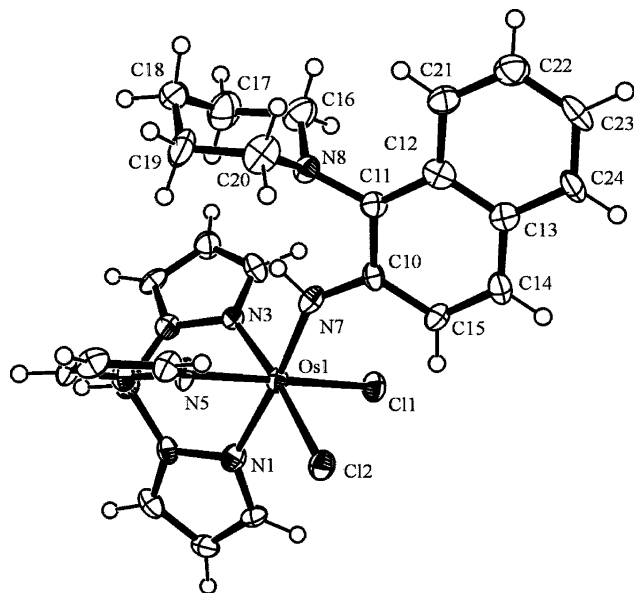
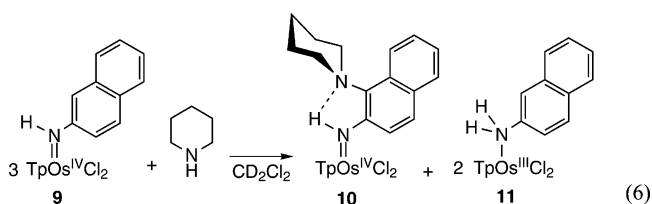


Figure 2. ORTEP drawing of $\text{TpOs}[\text{NH}(2\text{-naphthyl-1-piperidyl})]\text{Cl}_2$ (**10**).

cannot have a contribution from a quinone diimine resonance form (Chart 1), which requires the lone pair to interact with the arene π system. There appears to be a hydrogen bond between this lone pair and the amide hydrogen because the N(8)···N(7) distance is 2.63 Å, and the N(8)···H(7) H-bond distance is ~ 2.11 Å.

The reactivity of **9** toward piperidine mimics that of **1**. Under aerobic conditions, the product forms in good yield (70%) over 1 week. In anaerobic conditions, the product forms in lower yields ($\sim 20\%$ after chromatographic workup with silica gel), and a new product, yellow NMR-silent **11**, is isolated by chromatography in 55% yield. A solution of **11** in CD_2Cl_2 in air converts over a week to **9**, as indicated by ^1H NMR and the deep purple color. These properties are analogous to those of **5**, suggesting that **11** is $\text{TpOs}^{\text{III}}(\text{NH}_2\text{-2-naphthyl})\text{Cl}_2$. Consistent with this assignment, FAB^+/MS spectra of **11** show $m/z = 619$ ($[\text{M} - \text{H}]^+$). The anaerobic reaction is thus well described by eq 6. $\text{TpOs}[\text{NH}(1\text{-}$



naphthyl)] Cl_2 also reacts with piperidine, but no products were observed by ^1H NMR. Column chromatography on silica gave three materials in low yield that could not be characterized.

Ab Initio Studies of $\text{TpOs}(\text{NHPh})\text{Cl}_2$ (1**).** Ab initio calculations have been performed on **1** to examine the nature of the frontier molecular orbitals. Starting from the X-ray crystal structure of **1**^{5a} the molecular geometry was optimized, in C_s symmetry, at the RHF level using the LANL2DZ basis set. Vibrational analysis confirmed that the optimized C_s structure is a minimum. The LUMO (Figure 3) is of particular interest in light of the nucleophilic attack on **1**. It

- (23) (a) Miller, J. *Aromatic Nucleophilic Substitution*; Elsevier: New York, 1968 (the quote is from p 209). (b) Buncl, E.; Crampton, M. R.; Strauss, M. J.; Terrier, F. *Electron Deficient Aromatic- and Heteroaromatic-Base Interactions*; Elsevier: New York, 1984. (c) Terrier, F. *Nucleophilic Aromatic Displacement: The Influence of the Nitro Group*; VCH: New York, 1991. (d) March, J. *Advanced Organic Chemistry*, 4th ed.; Wiley: New York, 1992; pp 641–644. (e) Makosza, M.; Winiarski, J. *Acc. Chem. Res.* **1987**, *20*, 282–289. (f) Makosza, M.; Kwast, A. *J. Phys. Org. Chem.* **1998**, *11*, 341–349. (g) Chapakhin, O. N.; Charushin, V. N.; Van der Plas, H. C. *Nucleophilic Aromatic Substitution of Hydrogen*; Academic Press: New York, 1984.
- (24) (a) Lawrance, G. A. *Chem. Rev.* **1986**, *86*, 17–33. (b) Mahon, M. F.; Whittlesey, M. K.; Wood, P. T. *Organometallics* **1999**, *18*, 4068–4074. (c) Veghini, D.; Berke, H. *Inorg. Chem.* **1996**, *35*, 4770–4778. (d) Conry, R. R.; Mayer, J. M. *Organometallics* **1993**, *12*, 3179–3186.

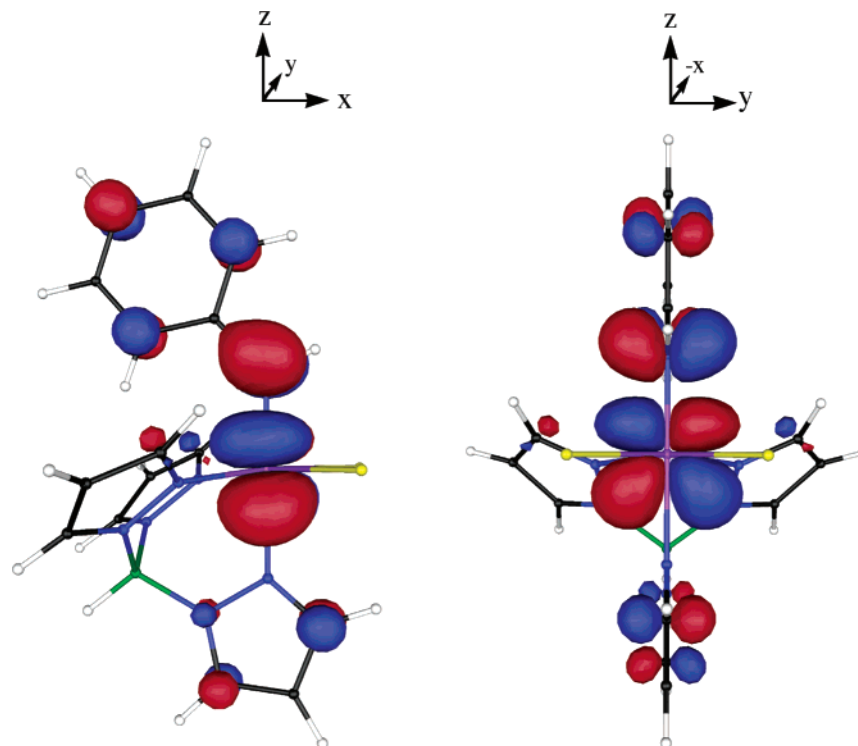
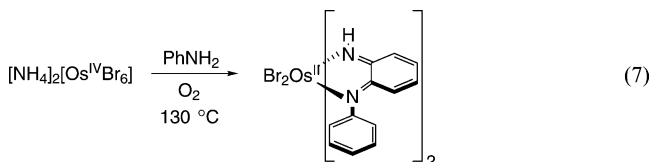


Figure 3. Plots of the LUMO in **1** from RHF/LANL2DZ calculations, shown in two orientations rotated by 90° about the vertical.

is localized primarily on the osmium and the anilido ligand and shows a π -antibonding interaction between the Os d_{yz} orbital and the p_π orbital on the anilido nitrogen (p_y). The π^* character of the LUMO supports the presence of significant Os–N π bonding in **1**. Complexes with metal–ligand multiple bonds typically have π^* LUMOs.³ There is also substantial LUMO orbital density on the anilido aromatic ring at both the *ortho* and *para* positions. This provides a rationale for the observed electrophilic reactivity of the aromatic rings in **1** and **9**.

Discussion

The formation of ring-substituted products from reactions between arylamido osmium complexes (**1**, **7**, **9**) and amines is very unusual. The most closely related processes are the arylamine coupling reactions promoted by osmium, ruthenium, and rhodium salts reported by Goswami et al.¹⁹ These reactions generate *o*-quinone diimine chelates at high temperatures in the presence of O₂ from primary arylamines such as aniline (e.g., eq 7). The stoichiometries of these reactions



are typically not known, and their mechanisms are poorly defined. The reactions described here afford a unique opportunity to examine metal-assisted aromatic substitution reactions in detail.

Mechanism of Formation of Ring-Substituted Materials. 1. Initial Steps. The initial step(s) in these reactions

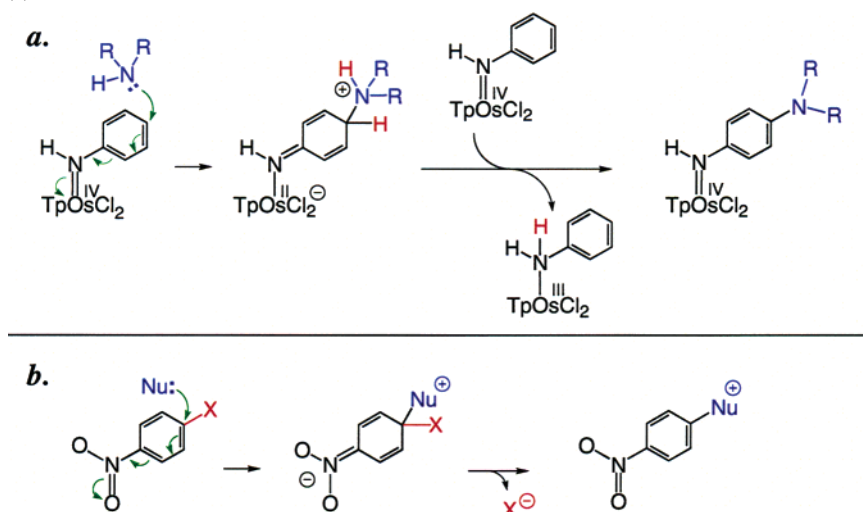
could be nucleophilic attack or initial electron transfer followed by a radical coupling. The latter pathway, outer-sphere electron transfer from the amine to the osmium, is ruled out by the redox potentials involved. Complex **1** is not a good outer-sphere oxidant ($E_{1/2} = -1.05$ V vs Cp₂Fe⁺⁰ in CH₃CN),¹¹ in contrast to other TpOs^{IV}(X)Cl₂ complexes that have potentials at or above Cp₂Fe⁺.¹⁶ Electron transfer to **1** from piperidine or pyrrolidine ($E_{1/2} = 0.67$ and 0.60 V, respectively²⁵) is uphill by >1.6 V or >37 kcal mol⁻¹. This is larger than the measured ΔG^\ddagger of 21 kcal mol⁻¹ at 298 K, eliminating this as a reasonable pathway. In addition, **1** does not react with diphenylamine, which has a much lower redox potential than the dialkylamines, $E_{1/2} = -0.12$ V vs Cp₂Fe⁺⁰ in DMSO.²⁶

The indicated mechanism for the reactions described here therefore involves initial addition of the nitrogen base to the aromatic ring (Scheme 1a). This is analogous to organic nucleophilic aromatic substitution (S_NAr) reactions.²³ Aromatic rings are activated toward nucleophilic attack by electron-withdrawing substituents, such as the nitro group in Scheme 1b. In a formal sense, the nitro group receives two electrons upon addition of the nucleophile. In the osmium chemistry, the TpOs^{IV}Cl₂ fragment accepts the two electrons, generating a zwitterionic Os^{II} intermediate. This intermediate resembles the Os^{II} quinone diimine resonance form for substituted products as drawn in Chart 1, suggesting that it is energetically reasonable.

The mechanism in Scheme 1a also provides an explanation for the unusual activation parameters observed in reaction of **1** with pyrrolidine. The formation of charged intermediates

(25) Liu, W.-Z.; Bordwell, F. G. *J. Org. Chem.* **1996**, *61*, 4778–4783.

(26) Bordwell, F. G.; Zhang, X.; Cheng, J.-P. *J. Org. Chem.* **1991**, *56*, 3216–3219.

Scheme 1. Mechanism for Nucleophilic Aromatic Substitution for Osmium(IV) Arylamides (a) and Comparison with S_NAr Reactions of Nitroaromatic Compounds (b)

from neutral precursors requires significant organization of solvent in the transition state, the likely cause of the large negative entropy of activation ($\Delta S^\ddagger = -80 \pm 20$ eu). This effect has also been observed in organic S_NAr processes, as summarized in the book *Aromatic Nucleophilic Substitution*: “[An] important feature is that the values of ΔS^\ddagger for reactions of neutral nucleophiles with neutral substrates [as in Scheme 1] are much more negative than those for reactions of anionic nucleophiles...”²³ The activation entropies for organic reactions are not as negative as for **1** + pyrrolidine, but reaction of piperidine with 1-chloro-2,4-dinitrobenzene in benzene has $\Delta S^\ddagger = -44$ eu and $\Delta H^\ddagger = 6$ kcal mol⁻¹ (in MeOH, $\Delta S^\ddagger = -30$ eu).^{23a} Additionally, rates of organic S_NAr processes between neutral reactants are significantly diminished in benzene relative to polar aprotic solvents, ascribed to better solvation of the charge-separated transition state.²³ The reaction of **1** + pyrrolidine has the same properties: a small ΔH^\ddagger , a large negative ΔS^\ddagger , and a reaction rate ~ 4 times slower in 60/40 MeCN/C₆H₆ than in pure MeCN.

Nucleophilic reactions such as in Scheme 1 proceed faster with more nucleophilic reagents. Unfortunately, there is no simple and complete nucleophilicity scale, quantitative or qualitative.²⁷ One review, for instance, lists *in summary* 17 factors that may influence nucleophile reactivity.²⁸ For amines, the two most important factors seem to be basicity and sterics, and the relative rates of reaction with **1** can be understood on this basis. Pyrrolidine is more basic than piperidine ($pK_a = 19.6$ vs 18.9)²¹ and its lone pairs are more exposed, so it reacts nearly 3 times faster at 298 K. Morpholine is sterically similar to piperidine but has a significantly lower pK_a (16.6) and reacts orders of magnitude slower. The absence of reactivity with aniline (10.7) or pyridine (12.3) is likely due to their low basicity. Diethylamine (18.7) is likely unreactive because of unfavorable

steric interactions, but reaction does occur with the smaller and comparably basic MeNH₂ (18.4).²¹

Mechanism of Formation of Ring-Substituted Materials. 2. Hydrogen Removal. Typical nucleophilic aromatic substitution (S_NAr) reactions involve displacement of halogens or other nucleofugal leaving groups.²³ The reactions presented here are unusual in that they involve formal nucleophilic substitution of hydride. Organic examples of such hydrogen substitutions have been studied in detail by the groups of Makosza and van der Plas.^{23e-1} These reactions require an oxidizing agent, such as O₂ or KMnO₄, to rearomatize the intermediate (equivalently to remove the “hydride” leaving group). Nitroarenes can function both as substrate and as oxidant (“spontaneous” oxidations) so that substituted products are obtained in low yields versus nitroarene consumed.^{23e-g} In the osmium reactions, 2 equiv of **1** or **9** acts as oxidizing agent, so the maximum yield of substituted products is only 33%, unless O₂ is present.

The oxidation of the Os^{II} zwitterionic intermediate occurs by loss of two hydrogen atoms (two protons and two electrons). Each hydrogen is transferred to **1**, forming 2 equiv of the Os^{III} aniline complex **5** per substituted product. Such reactions in which a metal complex abstracts a hydrogen atom have been a focus of our group for some time,²⁹ and the intrinsic H-atom transfer reactivity of **1** and **5** has been investigated.¹² A key parameter in such reactions is the thermochemical affinity of the oxidant for H[•], in this case the N–H bond strength in **5**, which has been shown to be 66 kcal mol⁻¹.¹³ Hydrogen atom removal does not appear to be rate-limiting in the piperidine or pyrrolidine reactions, on the basis of the absence of a kinetic isotope effect in the reaction of TpOs(NHPh-*d*₅)Cl₂ (**1-d**₅) with pyrrolidine-1-*d*. In addition, the parallel between the rates of reaction and the apparent nucleophilicity of the amine suggests that the amine addition is rate-determining. With morpholine, however, the more complex kinetics and normal temperature

(27) See: *Nucleophilicity*; Harris, J. M., McManus, S. P., Eds.; *Advances in Chemistry* 215; American Chemical Society: Washington, DC, 1987.

(28) Bunnett, J. F. *Ann. Rev. Phys. Chem.* **1963**, 14, 271–290.

(29) (a) Mayer, J. M. *Acc. Chem. Res.* **1998**, 31, 441–450. (b) Roth, J. P.; Yoder, J. C.; Won, T.-J.; Mayer, J. M. *Science* **2001**, 294, 2524–2526.

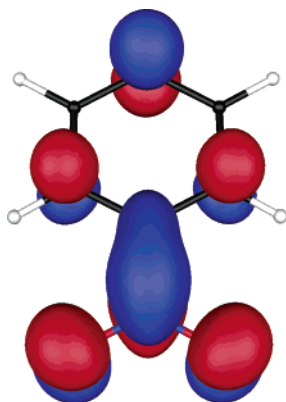


Figure 4. Plot of the LUMO in nitrobenzene from RHF/LANL2DZ calculations.

dependence of the rates could indicate a change in the rate limiting pathway, perhaps with hydrogen transfer being kinetically important.

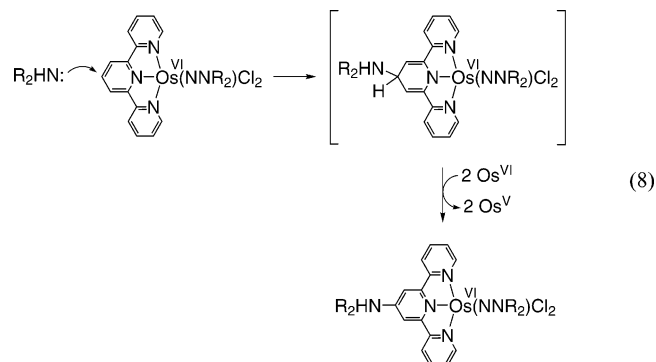
The osmium reactions are not limited to displacement of hydride. The reaction of the *p*-chloroanilide **7** with piperidine gives quantitative conversion to **2**, without formation of the aniline complex **5**. This is a typical S_NAr reaction where the nucleophile displaces a good leaving group. High yields are obtained because an oxidant is not required—because the presumed intermediate rearomatizes simply by loss of chloride. It is interesting that displacement of chloride is much slower than displacement of hydrogen (weeks vs 2 days). This could be a steric effect, with the large chlorine atom inhibiting nucleophile addition, or π -donation from Cl to the electron-deficient aromatic ring may stabilize the ground state of **1** more than the transition state.

Electrophilic Reactivity of Os(IV) Arylamide Ligands.

The ab initio calculations on $TpOs(NHPh)Cl_2$ (**1**) indicate the origin of the electrophilic reactivity. The LUMO of **1** (Figure 3) is Os–N π -antibonding and has a surprising amount of density on the arene ring, the site of nucleophilic attack. The portion of the LUMO on the arene ring bears a striking resemblance to the LUMO in nitrobenzene (Figure 4, calculated at the same level of theory as Figure 3). Nitrobenzene is also prone to nucleophilic attack at the *ortho* and *para* positions.²³ For the osmium compounds, addition to the arene ring is also much less sterically demanding than addition to the osmium or the amido nitrogen. This steric advantage is a general feature of reactions that occur at ligands rather than at the metal center. Steric effects are presumably the reason complex **1** adds nucleophiles preferentially at the *para* position. When the *para* position is blocked, as in the *p*-tolyl and naphthyl derivatives, nucleophilic attack appears to occur on the basis of color changes, but only in the case of **9** has an *ortho*-substituted product been isolated.

To our knowledge these are the first clear examples of a transition metal activating an aryl amido ligand toward nucleophilic attack. Similar activation may be involved in the aniline reactions examined by Goswami and co-workers (e.g., eq 7 above).¹⁹ These reactions involve umpolung, inversion of chemical character,⁴ as the arylamido ligand is normally an electron-rich arene, susceptible to electrophilic

attack. This electrophilic character can be enhanced by metal complexation, as shown for electron-rich rhodium dimers by Ge and Sharp.³⁰ The nucleophilic reactions described here should be contrasted with the recently reported nucleophilic substitution of a *para* hydrogen of a terpyridine ligand on an Os^{VI} hydrazido complex (eq 8).^{6d} This proceeds by initial



nucleophilic attack of the amine on the pyridine ring (although an electron-transfer mechanism was first suggested^{6e}). The subsequent rearomatization requires 2 equiv of the starting material acting as one-electron oxidants, as in Scheme 1a. However, the initial attack at the pyridine is *not* a redox reaction at osmium and the function of the metal in this step is solely as a Lewis acid. Nucleophilic attack at coordinated and free pyridines is common,^{23a–d} and eq 8 is not an example of umpolung.

The features of these compounds that promote nucleophilic attack are (i) Os^{IV} is a good two-electron oxidant and (ii) this redox change is coupled to changes in the bonding of the ligand. The Os^{IV} center has been referred to in this report as oxidizing, but as noted above it is not a good one-electron outer-sphere oxidant ($E_{1/2} = -1.05$ V vs $Cp_2Fe^{+/0}$). This is because an added electron must occupy the π^* LUMO. Analogous $TpOs^{IV}(X)Cl_2$ compounds in which the X ligand is not a strong π donor (Cl, O_2CCF_3 , triflate) have much higher redox potentials, at or above Cp_2Fe^+ .¹⁶ Reactions that convert the arylamido into a ligand that is not a π -donor will, in a sense, “reveal” this oxidizing power. Addition of a nucleophile serves this purpose, converting the arylamido into a σ -only imine donor (Scheme 1a). This coupling of redox change and bond formation is a characteristic of compounds with multiply bonded ligands.³ With these compounds, one-electron redox potentials are not a good predictor of bond-forming reactivity.

The ability of the Os^{IV} center to activate its arylamido ligand can apparently be tuned by changing the ancillary ligands. Upon replacing the chlorides with less donating triflate ligands, $TpOs(NHPh)(OTf)_2$ (**8**) reacts with amines within time of mixing rather than over a day or more for **1**. Such ancillary ligand effects are well-known for the reactivity of multiply bonding ligands, as in osmium(VI) nitrido complexes.^{5–7} The addition of Ph^- (as $PhMgBr$) to $TpOs(N)Cl_2$, for instance, is strongly inhibited by replacing Cl

(30) (a) Ge, Y.-W.; Sharp, P. R. *J. Am. Chem. Soc.* **1990**, *112*, 3667–3668. (b) Sharp, P. R. *J. Chem. Soc., Dalton Trans.* **2000**, 2647–2657. (c) Ge, Y.-W.; Sharp, P. R. *Inorg. Chem.* **1993**, *32*, 94–100.

for Ph, and this correlates with the calculated energies of the LUMOs.^{5a} This large effect of halide for hydrocarbyl substitution was first shown by Shapley and co-workers.^{7b} Related effects have been observed on comparing $\text{TpOs}(\text{N})\text{Cl}_2$, $[(\text{tpy})\text{Os}(\text{N})\text{Cl}_2]^+$, and $[(\text{Tpm})\text{Os}(\text{N})\text{Cl}_2]^+$.^{6,7}

Conclusions

The oxidizing and electrophilic $\text{TpOs}^{\text{IV}}\text{Cl}_2$ fragment activates arylamido ligands toward remarkable nucleophilic aromatic substitutions ($\text{S}_{\text{N}}\text{Ar}$) of hydrogen. This is an inversion of reactivity (umpolung) because arylamido ligands are typically electron-rich and susceptible to electrophilic attack. The electrophilic character of the anilido ligand in $\text{TpOs}^{\text{IV}}(\text{NHPh})\text{Cl}_2$ (**1**) is indicated by calculations that show a low-lying LUMO with substantial density on the phenyl ring, similar to the LUMO of nitrobenzene. The rates of secondary amine addition to the phenyl ring of **1** parallel the nucleophilicity of the base, with smaller and more basic amines reacting more rapidly. Amine addition forms a putative Os^{II} -iminocyclohexadiene intermediate, and an oxidant is required to rearomatize the aryl ring (Scheme 1a). Under anaerobic conditions, $\text{TpOs}^{\text{IV}}(\text{NHAr})\text{Cl}_2$ itself serves as the oxidant, abstracting a hydrogen atom to form $\text{TpOs}^{\text{III}}(\text{NH}_2\text{Ar})\text{Cl}_2$ (**5**). Alternatively, O_2 can serve as the oxidant, because it oxidizes **5** back to **1**. The ability of the Os^{IV} center to activate coordinated ligands is traced to its two-electron oxidizing power and is not indicated by its modest redox potential. Redox change at osmium is coupled to chemical change at the ligand as a result of the $\text{Os}-\text{NHAr}$ π bonding. The ability of oxidizing metal centers to activate coordinated ligands is a topic of ongoing investigation in our laboratory.

Experimental Details

General Considerations. All manipulations were performed under anaerobic conditions using standard high-vacuum and nitrogen-filled glovebox techniques unless otherwise noted. NMR spectra were acquired on Bruker WM-500, DRX-499 and AF-300 spectrometers at 298 K. ^1H NMR chemical shifts were referenced to the residual ^1H NMR signals of the solvent and are reported versus TMS. ^{19}F NMR chemical shifts are referenced to external CFCl_3 . UV-vis spectra were obtained using a HP 8453 UV-vis spectrophotometer and are reported as λ_{max} [nm] (ϵ [$\text{M}^{-1}\text{cm}^{-1}$]). IR spectra were obtained as either KBr pellets or CH_2Cl_2 solutions using a Perkin-Elmer 1720 FTIR spectrophotometer. Electrospray ionization mass spectrometry was carried out in MeCN using a Bruker/HP Esquire-LC mass spectrometer. FAB⁺/MS data were obtained using a JEOL HX 110 double focusing sector mass spectrometer (3-nitrobenzyl alcohol matrix, Xe). Elemental analyses were performed by Atlantic Microlab, Inc. in Norcross, GA. Kinetics data were fit with SpecFit from Spectrum Software Associates.

Materials. All solvents were degassed and dried according to standard procedures.³¹ CH_3CN was used as obtained from Burdick and Jackson (low-water brand) in an argon-pressurized stainless steel drum (plumbed directly into a glovebox). Deuterated solvents (Cambridge Isotope Laboratories) were degassed, dried, and vacuum

transferred prior to use. CDCl_3 and CD_2Cl_2 were dried over CaH_2 . CD_3CN was dried by successively stirring over CaH_2 , followed by P_2O_5 and again over CaH_2 to remove trace acids. Other reagents (Aldrich) were used as received unless otherwise noted. Piperidine, pyrrolidine, and morpholine were distilled from sodium metal prior to use. Anilines were distilled from KOH or CaH_2 under reduced pressure and thoroughly degassed prior to use. $\text{TpOs}(\text{N})\text{Cl}_2$,^{5a} $\text{TpOs}(\text{NH}_2\text{Ph})\text{Cl}_2$ (**5**),¹³ $\text{TpOs}(\text{NHPh})\text{Cl}_2$ (**1**),^{5c} $\text{TpOs}(\text{NHPh-}d_3)\text{Cl}_2$ (**1-}d_3**),^{11b} $\text{TpOs}(\text{NHPh})(\text{OTf})_2$ (**7**),^{11a} and $\text{TpOs}(\text{NHTol})\text{Cl}_2$,^{5a,11b,17} were prepared according to published procedures.

$\text{TpOs}[\text{NH-}p\text{-C}_6\text{H}_4(c\text{-NC}_5\text{H}_{10})]\text{Cl}_2$ (2**).** A glass flask with a Teflon stopcock was charged with **1** (40 mg, 70 μmol), CH_3CN (4.0 mL), and piperidine (21 μL , 212 μmol). The flask was cooled to -196 °C and charged with O_2 . (**Caution: condensing liquid oxygen in the presence of organics is potentially explosive.**) After 19 d at ambient temperatures, the bright blue solution was reduced to dryness in vacuo. The residue was dissolved in minimal CH_2Cl_2 , and column chromatography in air (silica, 90% $\text{CH}_2\text{Cl}_2/10\%$ acetone) followed by recrystallization from acetone/pentane gave blue **2** (29 mg, 45 μmol , 64%). ^1H NMR (CD_3CN): δ 6.15 (br, 2H), 3.76 (br, 2H) (*NPh m, o*); 15.5 (br s, 1H, *NHPh*); 4.31 (t, 5.5 Hz, 4H), 1.74 (br m, 2H), 1.63 (br m, 4H) (*c-NC}_5\text{H}_{10}*); 6.39 (t), 7.72 (d), 6.88 (d) (all 1H, 2 Hz, pz); 6.42 (t), 6.69 (d), 6.21 (d) (all 2H, 2 Hz, pz'). FAB⁺/MS: 650 (M^+). IR (KBr): 3478 (br) ($\nu_{\text{N-H}}$); 2526 (m) ($\nu_{\text{B-H}}$); 3215 (m); 2935 (w); 2845 (w); 1700 (m); 1591 (s); 1518 (m); 1370 (m); 1356 (m); 1241 (s); 1093 (m); 1018 (m); 914 (w); 883 (w); 788 (m); 777 (m). UV-vis (MeCN): 600 nm (30 000). Anal. Calcd (Found) for $\text{C}_{20}\text{H}_{25}\text{BCl}_2\text{N}_8\text{Os}\cdot\text{C}_3\text{H}_6\text{O}$ [1 equiv of acetone is observed in the X-ray structure and in ^1H NMR spectra of **2** after recrystallization] C: 39.05 (39.29, 39.14), H: 4.42 (4.56, 4.54), N: 15.84 (15.82, 15.73).

$\text{TpOs}[\text{NH-}p\text{-C}_6\text{H}_4(c\text{-NC}_4\text{H}_8)]\text{Cl}_2$ (3**).** Following the procedure described for **2**, 25 mg of **1** (44 μmol) and 12 μL of pyrrolidine (140 μmol) gave, after 6 d at ambient temperatures and similar chromatographic workup and recrystallization, 21 mg of blue **3** (33 μmol , 77%). ^1H NMR (CD_3CN): δ 5.85 (br, 2H), 4.37 (br, 2H) (*NPh m, o*); 16.0 (br s, 1H, *NHPh*); 5.40 (br m, 4H), 1.85 (br m, 4H) (*c-NC}_4\text{H}_8*); 6.41 (t), 7.77 (d), 6.98 (d) (all 1H, 2 Hz, pz); 6.39 (t), 6.80 (d), 6.16 (d) (all 2H, 2 Hz, pz'). ESI-MS: 659 ($\text{M} + \text{Na}^+$), 675 ($\text{M} + \text{K}^+$). IR (KBr): 3439 (br) ($\nu_{\text{N-H}}$); 2526 (m) ($\nu_{\text{B-H}}$); 3098 (w), 1496 (m), 1401 (s), 1314 (m), 1213 (m), 1113 (m), 1046 (s), 987 (w), 760 (m), 710 (m), 648 (w), 618 (w) (all Tp); 3215 (m); 2946 (w); 2851 (w); 1703 (m); 1594 (s); 1521 (m); 1474 (m); 1454 (w); 1339 (m); 1253 (w); 1093 (m); 1018 (m); 953 (w); 833 (w); 788 (m); 777 (m). UV-vis (MeCN): 596 nm (25000). Anal. Calcd (Found) for $\text{C}_{19}\text{H}_{23}\text{BCl}_2\text{N}_8\text{Os}\cdot\text{C}_3\text{H}_6\text{O}$ [1 equiv of acetone is observed in ^1H NMR spectra of **3** after recrystallization]. C: 38.10 (38.35, 38.47), H: 4.22 (4.36, 4.25), N: 16.16 (16.28, 16.14).

Other Substituted Anilido Products. Addition of excess MeNH_2 or morpholine to NMR tubes containing **1** in CD_3CN gives ^1H NMR spectra consistent with formation of *para*-substituted materials and **5** in ~30% and ~65% yields, respectively. The complexes were isolated in small amounts by column chromatography on silica in air using 5% acetone/ CH_2Cl_2 . **-NHMe:** After 6 d at ambient temperatures under 1 atm of MeNH_2 , color change from dark red to purple was observed. ^1H NMR (CD_3CN): δ 5.88 (br, 2H), 4.0 (br, 2H) (*NPh m, o*; *NHPh* not observed); 4.15 (d, 5 Hz, 3H), 3.9 (br m, 1H) (*-NHCH}_3*); 6.41 (t), 7.76 (d), 6.94 (d) (all 1H, 2 Hz, pz); 6.41 (t), 6.74 (d), 6.22 (d) (all 2H, 2 Hz, pz'). **-(c-NC}_4\text{H}_8\text{O}) (**4**):** With 3 equiv of morpholine, after 15 d at ambient temperatures and 11 d at 80 °C, color change to bright blue was observed. ^1H NMR (CDCl_3): δ 6.4 (br, 2H), 6.2 (br, 2H) (*NPh m, o*); 12.5 (br s, 1H, *NHPh*); 4.80 (t), 3.67 (t), (both 4H, 7

(31) Perrin, D. D.; Armarego, W. L. F. *Purification of Laboratory Chemicals*, 3rd ed.; Pergamon: New York, 1988.

Hz, 5 Hz, (*c*-NC₄H₈O)); 6.29 (t), 7.31 (d), 6.70 (d) (all 1H, 2 Hz, pz); 6.44 (t), 6.10 (d) (all 2H, 2 Hz, pz'; one doublet not observed). UV-vis (CH₃CN): 625 nm. ESI-MS: 651 (M⁺).

TpOs(NH-*p*-C₆H₄Cl)Cl₂ (6). A glass flask with a Teflon stopcock was charged with TpOs(N)Cl₂ (151 mg, 309 μmol), CH₂-Cl₂ (10 mL), and 4-chloroaniline (120 mg, 957 μmol) and heated at 80 °C for 5 days. The dark red solution was worked up by column chromatography in air (silica, 90% CH₂Cl₂/10% acetone) and recrystallization from acetone/pentane, yielding red/orange **6** (29 mg, 48 μmol, 15%). ¹H NMR (CD₃CN): δ 8.99 (d, 9.4 Hz, 2H), 2.55 (br s, 2H) (*NPh m, o*); 6.23 (t), 6.04 (d), 5.07 (d) (all 1H, 2.3 Hz, pz); 6.67 (t), 7.21 (d), 4.71 (d) (all 2H, 2.3 Hz, pz'). ESI-MS: 602 (M + H⁺), 640 (M + K⁺). IR (KBr): 3467 (br) (*ν*_{N-H}); 2504 (m) (*ν*_{B-H}); 3120 (w), 1496 (m), 1404 (s), 1311 (m), 1208 (m), 1186 (s), 1118 (m), 1071 (m), 1048 (s), 987 (w), 763 (m), 707 (m), 654 (w), 615 (m) (all Tp); 2918 (w); 2851 (w); 1700 (m); 1566 (m); 1387 (m); 1093 (m); 1012 (w); 917 (w); 833 (w); 811 (w); 788 (m). Anal. Calcd (Found) for C₁₅H₁₅BCl₃N₇O₈·1/3(C₅H₁₂) [one-third of a molecule of pentane is observed in the ¹H NMR after recrystallization]. C: 31.85 (31.89, 31.75), H: 3.01 (3.19, 3.08), N: 15.75 (15.75, 15.61).

TpOs[NH-(1-naphthyl)]Cl₂. 1-Naphthylmagnesium bromide (0.25 M in THF, 860 μL, 0.216 mmol, 1.00 equiv) was added dropwise to a -32 °C solution of TpOs(N)Cl₂ (105.4 mg, 0.216 mmol) in ~15 mL of THF. The reaction mixture was cooled to -78 °C and quenched with ~1 mL of distilled water. Solvent removal, chromatography (silica gel, 100:1 CH₂Cl₂/acetone), and recrystallization (hexanes/CH₂Cl₂) yielded TpOs[NH-(1-naphthyl)]-Cl₂ (24.1 mg, 18%) as a gray-blue solid. ¹H NMR (CD₂Cl₂): 9.71, 8.61 (t, 1H each, 7 Hz) (3,6-*CH*); 7.98 (d, 9 Hz, 1H, 8-*CH*), 6.90 (d, 2 Hz, 2H, Tp), 6.75 (t, 2 Hz, 2H, Tp), 6.24 (d, 2 Hz, 1H, Tp), 6.02 (t, 2 Hz, 1H, Tp), 4.98 (d, 2 Hz, 1H, Tp), 4.25 (d, 2 Hz, 2H, Tp), 3.3 (br s, 1H, *NH*), 5.16, -4.2, -10.1 (d, each 1H, 2,4,5-*CH*), 4.15 (t, 1H, 7-*CH*). IR: 3279 (NH), 3125, 3049, 2991 (CH); 2515 (BH); 1651, 1614, 1557, 1504, 1406, 1312, 1266, 1211, 1117, 1050, 991, 926, 887, 816, 791, 762, 734, 709, 652, 617. UV-vis: 570 (4000), 461 (3000), 422 (3100), 320 (9000). ESI/MS: 656 (M + K⁺), 640 (M + Na⁺), 616 (M⁺). Anal. Calcd (Found) for C₁₉H₁₈BCl₂N₇O₈: C, 37.03 (37.10); H, 2.94 (2.93); N, 15.91 (16.01)%.

TpOs[NH-(2-naphthyl)]Cl₂ (9). A two-neck 100-mL flame-dried flask was charged with 95.2 mg of TpOs(N)Cl₂ (0.195 mmol) and 15 mL of THF and cooled to -78 °C. A solution of 2-naphthylmagnesium bromide (390 μL of 0.5 M solution, 0.195 mmol, 1.00 equiv, diluted in 10 mL THF) was added dropwise over the course of 0.5 h. The reaction was then quenched at -78 °C by addition of ~1 mL of ambient temperature distilled water. Removal of the solvent, chromatography in air (silica, 100:1 CH₂-Cl₂/acetone) and recrystallized (layering hexanes over a CH₂Cl₂ solution) gave 54.1 mg of purple **9** (45%). ¹H NMR (CD₂Cl₂): 9.21 (d, 9 Hz, 1H, 5-*CH*), 9.00 (d, 8 Hz, 1H, 4-*CH*), 8.52 (t, 7 Hz, 1H, 7-*CH*), 6.83 (d, 2 Hz, 2H, Tp), 6.66 (t, 2 Hz, 2H, Tp), 6.30 (d, 2 Hz, 1H, Tp), 6.09 (t, 2 Hz, 1H, Tp), 5.22 (d, 2 Hz, 1H, Tp), 4.55 (d, 2 Hz, 2H, Tp), 4.3 (br s, 1H, *NH*), 3.47 (t, 7 Hz, 1H, 4-*CH*), 2.82 (d, 7 Hz, 1H, 8-*CH*), 0.30 (br s, 1H, 3-*CH*), -8.81 (br s, 1H, 1-*CH*). IR: 3235 (NH); 3144, 3049 (CH); 2514 (B-H); 1607, 1589, 1556, 1497, 1395, 1386, 1312, 1210, 1185, 1118, 1072, 1050, 990, 863, 814, 790, 765, 708, 617. UV-vis: 560 (9000), 446 (11000), 341 (7000), 286 (8000), 257 (14500), 212. FAB⁺/MS: 618 (M⁺), 583 (-Cl). Anal. Calcd (Found) for C₁₉H₁₈BCl₂N₇O₈: C, 37.03 (36.95); H, 2.94 (2.90); N, 15.91 (15.99).

TpOs[NH-(2-naphthyl-1-piperidine)]Cl₂ (10). In air, a 20 mL vial was charged with TpOs[NH-(2-naphthyl)]Cl₂ (55 mg, 0.089 mmol), CH₂Cl₂ (~5 mL), and piperidine (50 μL, 43 mmol, 500

equiv). The reaction was stirred in air for 1 week. Removal of the solvent and chromatography (silica gel, 100:1 CH₂Cl₂/acetone) yielded **10** (43.6 mg, 70%) as a green solid. Recrystallization (layering hexanes over a CD₂Cl₂ solution) yielded crystals suitable for X-ray analysis. ¹H NMR (CD₂Cl₂): 8.89 (d, 7 Hz, 1H), 8.68 (d, 8 Hz, 1H), 8.44 (t, 7 Hz, 1H), 8.28 (t, 7 Hz, 1H), 3.73 (d, 7 Hz, 1H) (naphthyl; one H not observed); 6.66 (d, 2 Hz, 1H), 6.65 (d, 2 Hz, 2H), 6.57 (t, 2 Hz, 2H), 6.16 (t, 2 Hz, 1H), 5.49 (d, 2 Hz, 1H), 5.10 (d, 2 Hz, 2H); (Tp), 3.6 (br s, 1H, *NH*), 3.4 (br, 4H), 2.2 (br, 2H), 2.0 (br, 4H) (pip). IR: 3450 (NH); 3123, 3040, 2934, 2851 (CH); 2509 (B-H); 1609, 1586, 1546, 1500, 1435, 1406, 1312, 1268, 1211, 1117, 1050, 989, 855, 815, 762, 734, 710, 654, 618. UV-vis: 633 (6400), 581 (7300), 459 (11000), 319 (16000). FAB⁺/MS: 700 (M⁺), 665 (-Cl), 614, 475, 224. Anal. Calcd (Found) for C₂₄H₂₇BCl₂N₈O₈: C, 41.21 (41.60); H, 3.89 (3.77); N, 16.02 (16.00).

Pyrrrolidine-1-*d*. *n*-Butyllithium (2.5 M in hexanes, 50 mL, 125 mmol) was added over 30 min to a vigorously stirring -78 °C solution of pyrrolidine (10 mL, 119 mmol; freshly distilled from sodium) in THF (10 mL). The reaction was stirred for 2.5 h at -78 °C and 1 h at ambient temperatures. The volatiles were removed in vacuo, and dropwise addition of methyl alcohol-*d* (4 mL, 98 mmol) to the resulting solids at -78 °C gave pyrrolidine-1-*d*, which was isolated by vacuum distillation. Isotopic enrichment as measured by ¹H NMR spectroscopy was >95%.

Kinetic Studies. In a representative procedure, 2.7 mL aliquots of a freshly prepared 4.7 × 10⁻⁵ M solution of **1** in CH₃CN were added to four quartz cuvettes fitted with Teflon stopcocks. To each cuvette was added 0.57 M pyrrolidine in CH₃CN (0.15 to 0.40 mL) such that the total concentration of pyrrolidine ranged from 30 to 73 mM. Reactions were monitored by UV-vis spectroscopy over 10 h at 25 °C. Data analysis is described in Results.

Computational Details. Calculations were performed using the GAUSSIAN 98 package of ab initio programs.³² Optimizations and vibrational analyses were performed at the restricted Hartree-Fock (RHF) level with the LANL2DZ basis set. As implemented in Gaussian 98 this basis set uses the D95V basis set³³ on H, B, C, and N, and the Los Alamos effective core potentials (ECP) plus DZ valence basis set on Cl³⁴ and Os.³⁵ Orbital plots were created using MacMolPlt.³⁶

Crystal Structures of TpOs[NH-*p*-C₆H₄(*c*-NC₅H₁₀)]Cl₂·acetone, TpOs[NH-*p*-C₆H₄(*c*-NC₄H₈)]Cl₂·CD₃CN, and TpOs[NH-(2-naphthyl-1-piperidine)]Cl₂ (10)·2·Acetone: A dark blue, prism-shaped crystal, size 0.24 × 0.17 × 0.05 mm³ was grown by slow diffusion of pentane into an acetone solution and mounted on a glass capillary in epoxy. **3·CD₃CN:** A dark blue crystal was cut

- (32) Frisch, M. J.; Trucks, G. W.; Schlegel, H. B.; Scuseria, G. E.; Robb, M. A.; Cheeseman, J. R.; Zakrzewski, V. G.; Montgomery, J. A., Jr.; Stratmann, R. E.; Burant, J. C.; Dapprich, S.; Millam, J. M.; Daniels, A. D.; Kudin, K. N.; Strain, M. C.; Farkas, O.; Tomasi, J.; Barone, V.; Cossi, M.; Cammi, R.; Mennucci, B.; Pomelli, C.; Adamo, C.; Clifford, S.; Ochterski, J.; Petersson, G. A.; Ayala, P. Y.; Cui, Q.; Morokuma, K.; Rega, N.; Salvador, P.; Dannenberg, J. J.; Malick, D. K.; Rabuck, A. D.; Raghavachari, K.; Foresman, J. B.; Cioslowski, J.; Ortiz, J. V.; Baboul, A. G.; Stefanov, B. B.; Liu, G.; Liashenko, A.; Piskorz, P.; Komaromi, I.; Gomperts, R.; Martin, R. L.; Fox, D. J.; Keith, T.; Al-Laham, M. A.; Peng, C. Y.; Nanayakkara, A.; Challacombe, M.; Gill, P. M. W.; Johnson, B.; Chen, W.; Wong, M. W.; Andres, J. L.; Gonzalez, C.; Head-Gordon, M.; Replogle, E. S.; Pople, J. A. *Gaussian 98*, Revision A.11.4; Gaussian, Inc.: Pittsburgh, PA, 2002.
- (33) Dunning, T. H., Jr.; Hay, P. J. In *Modern Theoretical Chemistry*; Schaefer, H. F., III, Ed.; Plenum: New York, 1976; Vol. 3, pp 1-28.
- (34) Hay, P. J.; Wadt, W. R. *J. Chem. Phys.* **1985**, *82*, 299.
- (35) Wadt, W. R.; Hay, P. J. *J. Chem. Phys.* **1985**, *82*, 284.
- (36) Bode, B. M.; Gordon, M. S. *J. Mol. Graphics Modell.* **1988**, *16*, 133-138.

from a rod that precipitated from a CD₃CN solution of **3**. The crystal was mounted on a glass capillary with oil. **10**: A dark green crystal, size 0.60 × 0.18 × 0.06 mm³ was grown by slow diffusion of hexanes into a solution in CH₂Cl₂ and mounted on a glass capillary with oil. Data were collected with one set of φ scans, at a crystal-to-detector distance of 27 (**2**), 35 (**3**), or 30 (**10**) mm, and with exposure times of 10 (**2**), 15 (**3**), or 30 (**10**) s, per degree for all sets. The scan widths were 1° (**2**, **10**) or 0.9° (**3**). Data collection to 25° in θ was 98.8% complete for **2**, 95.0% for **3**, and 96.7% for **10**. For **2**, a total of 46064 partial and complete reflections were collected, of which 6534 reflections were symmetry-independent (**3**: 25168 \Rightarrow 3987; **10**: 45261 \Rightarrow 5985). The R_{int} values of 0.0830 (**2**), 0.0351 (**3**), and 0.0802 (**10**) indicated that the data quality was excellent (**3**) and slightly less than average quality (0.07) (**2**, **10**). Indexing, unit cell refinement, and analysis of the normalized structure factors indicated the space groups given in Table 1. The data were integrated and scaled using *hkl*-SCALEPACK. This program applies a multiplicative correction factor (S) to the observed intensities (I) and has the following form: $S = \exp(2B(\sin \theta/\lambda)^2)/$ scale. S was calculated from the scale and B factor determined for

each frame and was then applied to I to give the corrected intensity (I_{corr}). Absorption corrections were performed numerically, using the redundancy of data. Solution by direct methods (SIR92) produced complete heavy atom phasing models consistent with the proposed structures. All non-hydrogen atoms were refined anisotropically by full matrix least-squares. All hydrogen atoms were located using a riding model.

Acknowledgment. This material is based upon work supported by the National Science Foundation under Grants 9816372 and 0204697. D.W. was also supported by an NSF REU award to the University of Washington Department of Chemistry. D.A.H. also thanks the National Science Foundation for support.

Supporting Information Available: Kinetic and crystallographic data. This material is available free of charge via the Internet at <http://pubs.acs.org>.

IC0498743